Glycinergic Feedback Enhances Synaptic Gain in the Distal Retina

Zheng Jiang[1*], Jinnan Yang[1], Lauren A Purpura[1], Yufei Liu[1],

Harris Ripps[2,3] and Wen Shen[1]

[1]Department of Biomedical Science, Charles E Schmidt College of Medicine, Florida Atlantic University, Boca Raton, Florida 33431, USA. [2]Department of Ophthalmology and Visual Sciences, University of Illinois College of Medicine, Chicago, IL 60612, USA, [3]Whitman Investigator, Marine Biological Laboratory, Woods Hole, MA 02543, USA

Running title: Glycine feedback enhances synaptic gain

Key Words: Salamander Retina, Glycinergic Interplexiform Cells, Synaptic Transmission

Figures: 8 **Words**: 5, 625

Correspondence: Dr. Wen Shen

Department of Biomedical Science

Charles E Schmidt College of Medicine,

Florida Atlantic University

Boca Raton, FL 33431

Email: wshen@fau.edu

[*]Current address: Department of Neuroscience, Johns Hopkins School of Medicine

Key Points:

1) This study provides experimental evidence that glycinergic interplexiform cells create a centrifugal feedback loop in the vertebrate retina that regulates the transmission of glutamatergic signals between photoreceptors and second-order neurons.

2) This mechanism serves to reduce glutamate uptake and enhance glutamate release.

3) Glycine receptors containing the GlyRα3 subunit are expressed on bipolar cell dendrites, and their activation leads to a depolarizing response in a group of rod-dominated ON-bipolar cells, and hyperpolarizing responses in OFF-bipolar cells.

4) Using strychnine to block endogenous glycine feedback reduces the amplitudes of light-evoked responses in both ON- and OFF-bipolar cells, indicating that glycine feedback regulates signal propagation in the distal retina.

5) Glycinergic feedback provides a neural mechanism that enhances synaptic gain and improves visual sensitivity.

Abstract

Glycine input originates with interplexiform cells, a group of neurons situated within the inner retina that transmit signals centrifugally to the distal retina. The effect on visual function of this novel mechanism is largely unknown. Using gramicidin-perforated patch whole-cell recordings, intracellular recordings, and specific antibody labeling techniques, we examined the effects of the synaptic connections between glycinergic interplexiform cells, photoreceptors, and bipolar cells. To confirm that interplexiform cells make centrifugal feedback on bipolar cell dendrites, we recorded the post-synaptic glycine currents from axon-detached bipolar cells while stimulating pre-synaptic interplexiform cells. The results show that glycinergic interplexiform cells activate bipolar cell dendrites that express the α3 subunit of the glycine receptor, as well as a subclass of unidentified receptors on photoreceptors. By virtue of their synaptic contacts, glycine centrifugal feedback increases glutamate release from photoreceptors, and suppresses the uptake of glutamate by the EAAT2 transporter on photoreceptors. The net effect is a significant increase in the synaptic gain between photoreceptors and their second-order neurons.

Abbreviations: DHKA, dihydrokainic acid; EAAT2A, the type 2A excitatory amino acid transporter; GlyRα3, glycine receptor α3 subunit**;** INL, inner nuclear layer; IPL, inner plexiform layer; LED, light emitting diode; OCT compound, Optimal Cutting Temperature compound; OPL, outer plexiform layer; TEA, tetraethylammonium

Introduction

In response to changes in ambient illumination, the vertebrate photoreceptor exhibits several unique features. In darkness, a sustained inward Na^+ flux depolarizes the cell and promotes the release of glutamate from vesicles in its synaptic terminal. When exposed to light, quantal absorption by the photopigment rhodopsin sets in motion a complex cyclic GMP-mediated cascade of biochemical reactions that reduces – in graded fashion - the discharge of transmitter. These opposing reactions provide visual information that is carried by parallel pathways to the innermost retina where it is received by ganglion cells for transmission to the brain. The parallel pathways originate in the outer plexiform layer (OPL) where photoreceptors make synaptic contact with horizontal and bipolar cells, the second-order neurons. Depending upon their voltage responses to light onset and offset, bipolar cells are classified as ON- or OFF-bipolar cells, each with properties that are critical for faithfully encoding the visual signals.

Of particular relevance to this research are the mechanisms that regulate the discharge of glutamate at the photoreceptor terminal. In particular, we propose to explore further earlier evidence that glycinergic feedback signals originating from interplexiform cells in the proximal retina increase the entry of Ca^{2+} into photoreceptor terminals, and thus enhance the release of neurotransmitter (Shen et al., 2008). This glycinergic feedback pathway has yet to be fully explored, and its functional significance is poorly understood. In this study, we examine how glycine affects glutamate uptake mediated by the excitatory amino acid membrane transporter type 2A (EAAT2A) expressed on photoreceptors. Its activity at these sites regulates the concentration of glutamate that reaches the bipolar cells (cf. Rowan et al., 2010). Here we show not only that glycinergic feedback signals and the fast glutamate uptake mechanism are participants in the regulation of glutamate within the photoreceptor's synaptic cleft, but that the two processes are governed by the same feedback mechanism.

These studies involve recordings of the synaptic release and uptake of glutamate by photoreceptors, and the light-evoked responses of bipolar cells in the salamander retina. Use of this amphibian model has two advantages: (i) the presence and physiological properties of glycinergic interplexiform cells in this species have been the subject of numerous studies (Smiley & Basinger, 1988; Yang & Yazulla, 1988; Maguire et al., 1990; Maple & Wu, 1998; Jiang & Shen, 2010), and (ii) their responses cannot be confounded with those mediated by other types of interplexiform cells (Dowling & Ehinger, 1978; Mangel & Dowling, 1987; Yang and Yazulla, 1988), since no other class of interplexiform cell has been detected in the amphibian retina.

Methods

All procedures were performed in accordance with the provisions of the National Institutes of Health Guide for the Care and Use of Laboratory Animals, and approved by the University's Animal Care Committee.

Retinal slice preparation

Tiger salamanders (*Ambystoma tigrinum*) were purchased from Kons Scientific (Germantown, WI) and Charles Sullivan (Nashville, TN). The animals were kept in aquaria at 13^{o}C under a 12-hour dark-light cycle with continuous filtration. After decapitation, the animals were double-pithed, and their eyes enucleated. Retinas, collected from animals kept in the dark for at least six hours, were placed in Ringer's solution and mounted on a piece of microfilter paper (Millipore, Bedford, MA) with the ganglion cell layer downward. Retinal slices were prepared in a dark room under a dissecting microscope equipped with powered Night-Vision scopes (BE Meyer Co., Redmond, WA). To avoid exposure to visible light, an infrared

illuminator (850 nm), an infrared camera, and a video monitor were used for tissue preparation. The filter paper with retina was vertically cut into 250 nm slices using a commercial tissue slicer (Stoelting Co, IL). A single retinal slice was mounted in a recording chamber and superfused with oxygenated Ringer's solution, consisting of (in mM): NaCl (111), KCl (2.5), $CaCl_2$ (1.8), $MgCl_2$ (1.0), HEPES (5.0) and dextrose (10), pH = 7.7. The recording chamber was placed on the stage of an Olympus BX51WI microscope equipped with a CCD camera linked to a monitor.

Electrophysiological recording

Whole-cell recordings were performed on bipolar cells, photoreceptors and interplexiform cells in dark-adapted retinal slices, using EPC-10 signal and dual amplifiers and HEKA Pulse software (HEKA Instruments Inc., Lambrecht/Pfalz, Germany). The phase angle setting was made with Pulse software based on the amplifier circuitry, and verified using a model cell. Patch electrodes (5–8 MΩ) were pulled with an MF-97 microelectrode puller (Sutter Instrument, Novato, CA). For experiments designed to determine the membrane current and light response of bipolar cells, the patch electrodes were filled with a high-potassium solution containing (in mM): K-gluconate (100); KCl (5); $MgCl_2$ (1); EGTA (5); HEPES (10); and an "ATP regenerating cocktails" consisting of (in mM): ATP (20) phosphocreatine (40) and creatinephosphotase (2); (pH = 7.4). The electrode solution resulted in a calculated E_{Cl} of -60mV. For whole-cell perforated-patch recordings, 2-3% of freshly prepared gramicidin A was added into the electrode solution. This polypeptide antibiotic forms transmembrane pores at the electrode tip that allows the passage of monovalent cations (Wallace, 1986), and prevents intracellular Cl^- concentration changes caused by dialysis of electrode solutions during conventional whole-cell recording.

Photic stimuli were delivered by a green LED (peak emission of 520nm) or white LED focused directly upon the retinal slice or whole-mount retinal tissue, and controlled by the output of the HEKA amplifier. The intensity of the stimulus was ~1.6 lux, which evoked both rod and cone activity. ON- and OFF-bipolar cells were identified by their light response patterns, and confirmed morphologically after dialyzing 3% Lucifer Yellow – a membrane impermeable fluorescent dye - through the recording electrodes.

Pairs of coupled photoreceptors/bipolar cells were patched simultaneously. The photoreceptor electrode contained (in mM): Cs-gluconate (50), Cs-glutamate (40), TEA (10), $MgCl_2$ (1), $CaCl_2$ (1), ATP-Mg (9), EGTA (5), GTP (0.5), HEPES (10mM), as published by Van Hook and Thoreson (2013); the bipolar cell electrodes contained (in mM): CsF (95), TEA (9.4), $MgCl_2$ (1.9), MgATP (9.4), EGTA (5.0), HEPES (12). A 300 msec depolarizing pulse was delivered to the photoreceptor, and the resultant synaptic current was recorded from the bipolar cell. Data were analyzed and plotted using Pulse and Igor/Excel software.

Capacitance measurements of exocytotic events were obtained from intact rods and cones in the slice preparation. The internal electrode solution consisted of (in mM) CsF (45); Cs-gluconate (50), TEA (10); $MgCl_2$ (2); MgATP (10); EGTA (1); HEPES (12); pH 7.2. The external Ringer solution consisted of $CsCl_2$ (10), TEA (20); NaCl (70); KCl (2.5); $CaCl_2$ (1.8); $MgCl_2$ (1); HEPES (5); dextrose (10); pH 7.7. The “lock-in” phase angle setting was made with Pulse software based on the EPC-10 amplifier circuitry, and verified with a model cell.

EAAT currents were recorded from photoreceptors using the same external solution, but the internal electrode solution was modified by replacing CsF and Cs-gluconate with an equivalent amount (95mM) of $CsNO_3$. Data were analyzed and plotted using Pulse and Igor/Excel software (WaveMetrics, Porland, OR, USA).

Intracellular recordings from bipolar cells were made with fine glass micropipettes drawn from single barrel ω-dot tubing on an MF-97 microelectrode puller (Sutter Instruments, Novato, CA). When filled with 2M potassium acetate, the resistance of the pipette was 100-200 MΩ, measured in Ringer's solution. A DC-coupled amplifier (Getting Instruments, San Deigo, CA) was used to record the voltage responses of bipolar cells. A gravity-driven system was used to superfuse solutions applied externally. The tip of the perfusion tube was placed 3 mm from the retinal slice and was manually controlled for delivering drugs during the experiments. For local glutamate application, an electrode having a tip diameter of 1mm diameter was filled with 1mM glutamate, placed at the IPL, and deposited by electrophoresis. To determine the charge across the bipolar cell membrane, the areas encompassed by the EPSCs were measured with Igor and Excel software (cf. Fig. 8D). Statistical data were generated with two-tailed T-test and expressed as mean $\pm$ SE. All chemicals used in this study were purchased from Sigma (St. Louis, MO) and Tocris (Minneapolis, MN).

Immunohistochemistry

Freshly enucleated eyes were fixed in a Ringer's solution containing 4% paraformaldehyde for 30 min. After removing the cornea and lens, the eyecup remained intact for further processing. It was then placed in the fixative for another 10 min, dehydrated in graded sucrose solutions (10%, 15%, 20% and 30%), and immersed in 30% sucrose overnight at 4^{o}C. The dehydrated eyecups were embedded in OCT compound (Ted Pella, Redding, CA), frozen overnight, and then sectioned at 12-18 μm on a cryostat. Frozen sections were collected on slides, air dried, and stored at -80°C. The dehydrated retinas were then prepared for immunostaining.

For antibody labeling, the sections were rinsed with 0.1% Tween and 0.3% Triton-X in PBS (PBST-T), and then treated with a blocking solution consisting of 5% normal goat or donkey serum and 0.1% sodium azide in PBS with 0.1% Tween (PBST). They were then incubated with a primary antibody mixture consisting of either 3% goat or donkey serum and 0.1% sodium azide in PBST-T overnight at 4^{o}C. Negative controls were performed with the same solutions, but lacking the primary antibody. After numerous washes with 0.1% sodium azide containing PBST, the sections were incubated in a fluorescent secondary antibody (Alexa 488 or Cy-3, each at a concentration of 1:600) for 40 minutes at room temperature. For double labeling, the second primary antibody was applied after single antibody labeling. Sections were subsequently rinsed with PBST, mounted with Vectorshield (Vector Laboratories, Burlingame, CA) and viewed with a confocal laser scanning microscope (LMS 700, Zeiss, Munich, Germany). Images were acquired with 40x and 63x oil-immersion objectives, and then processed with Zen software. The anti-GlyRα3 (rabbit polyclonal), anti-calretinin (goat polyclonal) and anti-$G_{o\alpha}$ (mouse monoclonal) were purchased from Chemicon (Billerica, MA, USA). The final concentrations used for anti-GlyRα3 1:1000; calretinin 1:8000 and $G_{o\alpha}$ 1:2000.

Results

Photic responses of glycinergic interplexiform cells

The morphology and neurophysiology of glycinergic interplexiform cells in the amphibian retina have been described in previous studies (Maguire et al., 1990; Jiang & Shen 2010). As illustrated in Fig. 1A, they show that the cell soma is located in the inner nuclear layer, and extend a long ascending process distally to the OPL. Earlier studies also revealed that glycinergic interplexiform cells receive both excitatory and inhibitory inputs from glutamatergic

bipolar cells and glycinergic/GABAergic amacrine cells, respectively. As a result, photic stimulation of interplexiform cells evokes transient depolarizing responses at light onset and offset (cf. Jiang & Shen 2010, Maguire et al., 1990). A typical recording from an interplexiform cell in the dark-adapted retinal slice preparation shows that, in response to a 3 sec exposure to a green stimulus (λ = 520 nm; I = 1.6 lux) that activated both rods and cones, the cell depolarized and fired an action potential at light onset, and gave a small depolarizing response at offset (Fig. 1B).

Evidence of glycinergic feedback on bipolar cell dendrites

To address the question of whether glycinergic interplexiform cells provide centrifugal feedback signals, we recorded current responses from axon-truncated bipolar cells marked with the fluorescent tracer Lucifer Yellow (Fig. 2A, upper). The schematic illustration (Fig. 2A, lower) shows the location in the IPL at which glutamate (1mM) was deposited electrophoretically. This preparation enabled us to activate interplexiform cells, while obviating any glycinergic input to the bipolar cells' axon terminals. ON- and OFF-bipolar cells in retinal slices were distinguished not only by the polarities of their light responses, but also by the location of their axon terminals: ON-bipolar terminals are located within sublamina *b* of the IPL, whereas the terminals of OFF-bipolar cells lie more distally in sublamina *a* of the IPL (Famiglietti & Kolb, 1976; Pang et al. 2004). After identifying the cell type, the axon terminal of the bipolar cell was carefully detached from the cell body with a sharp electrode, and the effect of glutamate was recorded in axon-truncated ON-bipolar cells that were voltage-clamped at 0mV. Figure 2B shows a sample recording in which a burst of synaptic currents were generated by activation of interplexiform cells; the currents were completely abolished when glycine receptors were blocked by strychnine (2 μM) applied in the bath solution, and partial

recovery of the current responses occurred after washout. In five successful recordings from axon-truncated bipolar cells, bursts of synaptic currents were generated, reflecting most probably the release of glycine from interplexiform cells.

Identity of the glycine receptor subtype expressed on bipolar cell dendrites

Antibodies against glycine receptor subunits, GlyRα1, GlyRα3, GlyRα4, were used to identify the type of glycine receptor expressed on bipolar cell dendrites. Of the various antibodies tested, only the one specific for the GlyRα3 subunit strongly labeled bipolar cells in the salamander retina. Expression of GlyRα3 on ON-bipolar cell dendrites can be seen in Fig. 3A where there is double-labeling of anti-GlyRα3 with an antibody against the G-protein subunit $G_{o\alpha}$, a marker for ON-bipolar cells. The two antibodies co-localized only on the dendrites of ON-bipolar cells in the OPL, but labeled individual axon terminals that ended separately within sublaminas *a* and *b* of the IPL (Fig. 3A, right).

The GlyRα3 antibody also labeled a group of neurons that resembled morphologically OFF-bipolar cells which, in salamander retina, have their somas both in the inner nuclear layer (INL), and at the inner margin of the outer nuclear layer (displaced bipolar cells, see double asterisks in Fig. 3B); in both cases, the axon terminals end at sublamina *a* of the IPL (Fig. 3B). The specificity of the antibody for the amphibian retina was verified in Western blot assays. The anti-GlyRα3 clearly recognized proteins at a molecular mass of 46 and 48 kDa in salamander and mouse retinal samples, respectively (Fig. 3C), consistent with the molecular mass (48 kD) of affinity purified GlyRα3. The somewhat smaller molecular mass for salamander GlyRα3 is probably due to a lesser degree of glycosylation, which may have occurred in post-translational modification of the receptor subunit.

Horizontal cells in the amphibian retina appear to lack GlyRα3 subunits, since double-labeling of anti-GlyRα3 and the antibody for calretinine, a horizontal cell marker in salamander retina, showed no overlap (Fig. 3D). Photoreceptors also appear to lack GlyRα3 subunits, although we have evidence that glycine enhances transmitter release from visual cells (see below).

Effects of glycine on bipolar cells

To demonstrate that glycine feedback in the OPL induces membrane potential changes in bipolar cells, we focally puffed glycine (100 μM) on the dendrites of intact bipolar cells in a slice preparation. The Ringer's solution bathing the preparation contained Cd^{2+} (100 μM) to block Ca^{2+}-dependent inputs from the network, and glycine-induced currents were recorded with gramicidin-perforated patch electrodes over a range of holding potentials (from -60mV to about -10 mV). After determining the glycine current reversal potential, a whole-cell recording configuration was achieved, and Lucifer Yellow was dialyzed through the pipette to reveal cell morphology. As already mentioned, the subgroups of ON- and OFF- bipolar cells in salamander retina can be differentiated by the location of their axon terminal endings within different sublaminas of the IPL. As shown by Pang et al. (2004) ON-bipolar cells receiving inputs predominately from rods having their axon terminals at the inner border of the IPL (Fig. 4A), whereas bipolar cells receiving cone-dominated inputs extend their axon terminals within the middle of the IPL. However, most bipolar cells receive inputs from both rods and cones and their axon terminals are present throughout the IPL (Figs. 4C, E). We used these morphological criteria as well as the polarities of their light-evoked responses to distinguish between the subgroups of bipolar cells.

Figure 4A shows typical current responses from a rod-dominated ON-bipolar cell whose axon terminal was located at the inner boundary (sublamina *b*) of the IPL. Note that the application of glycine on the dendrites of this bipolar cell generated inward and outward currents depending upon the voltage at which the cell was clamped; the voltage-current relationship showed a reversal potential around -37mV. The current reversal potentials for 13 of these ON-bipolar cells were distributed over a range of -30 to -45 mV (Fig. 4B). Since the dark membrane potentials of ON-bipolar cells are typically in the range of -45 to -60 mV, these neurons would tend to depolarize in response to a glycinergic input. Figure 4C shows results obtained from an ON-bipolar cell whose axon terminal ended in the middle of sublamina *b*, where it probably receives inputs from both rods and cones. In this case, the glycine puff at the OPL generated currents with a reversal potential around -46mV. The current reversal potentials for 27 ON-bipolar cells with similar morphology were within the range of -40mV to -55mV (Fig. 4D), both positive and negative to the dark membrane potential of ON-bipolar cells. Thus, many of these cells will depolarize in response to glycine, but it is difficult to predict what effect glycine might have on the remainder.

Similar protocols were applied to study glycine reversal potentials in a sub-group of OFF-bipolar cells whose terminals were located in sublamina *a*. The sample recording shown in Fig. 4E indicates that the glycine reversal potential was around -50mV. Glycine reversal potentials obtained from a similar group of OFF-bipolar cells (n = 29) are illustrated by the bar graphs in Figure 4F; most had glycine reversal potentials between -50mV and -60mV, i.e., negative to the neuron's dark membrane potentials that varied between -40mV to -30mV. In these cells, a glycinergic input would most likely elicit a hyperpolarizing response.

Glycine suppresses glutamate reuptake in photoreceptors

Earlier reports (Eliasof et al., 1998; Rowan et al., 2010) showed that EAAT2 is responsible for the re-uptake of glutamate at the synaptic membranes of photoreceptors and bipolar cells (Rowan et al., 2010). This Na^+- and K^+- dependent membrane transporter is capable of acting rapidly to limit the glutamate concentration in the OPL and its effect on bipolar cells. When the transporter takes up glutamate, an anion-mediated current is generated in the neuron (Arriza *et al.* 1997; Otis & Jahr, 1998). To study the effect of glycine on glutamate uptake in photoreceptor terminals, rods and cones were held at -60mV and subjected to a brief (2 ms) depolarizing step to -10mV; a 25 sec interval followed each depolarization. This protocol, used previously to study EAAT currents in salamander cone photoreceptors (cf. Rowan et al., 2010; Van Hook & Thoreson, 2012), served to activate voltage-dependent Ca^{2+} channels and to evoke glutamate release from photoreceptors. More importantly, it enabled us to record an anion-mediated EAAT current following vesicular release. An intracellular $CsNO_3$ was used in the pipette solution as the NO_3^- ion is more readily conducted by the transporters after glutamate binding.

The large, transient inward tail current (Fig. 5A, dark trace, arrow) that followed the capacitance spike was suppressed by DHKA (100μM), a selective inhibitor of EAAT2 (Fig. 5A, red trace). Of particular interest is the fact that glycine (50μM) also effectively reduced the EAAT currents in rods (Fig. 5B), and thus suppressed their ability to take up glutamate. The effect of glycine was completely eliminated by DHKA (Fig. 5C). Moreover, the effect of glycine on EAAT currents was blocked by strychnine (10μM) in the bath solution (Fig. 5D). These findings were replicated in several experiments (see n values in Fig. 5, and showed that glycine produced a significant ($p < 0.05$) reduction of ~42% in the EAAT2 uptake current (Fig. 5E).

Glycine also suppressed EAAT currents in cones, but to a lesser extent (Fig. 5F). DHKA inhibited EAAT2 and thereby blocked the effect of glycine on cones (Fig. 5G). On average, glycine suppressed 14 $\pm$ 0.06% of EAAT currents (n=7); DHKA blocked about 20% $\pm$ 0.05% (n=5) of EAAT currents in cones (Fig. 5H). Clearly, the actions of glycine on glutamate uptake in rods and cones will enhance considerably the glutamate content in the synaptic cleft, and increase glutamate activation of bipolar cells.

Effects of glycine input on glutamate release

To determine whether glycinergic feedback also regulates the vesicular release of glutamate at the photoreceptor terminal, we measured membrane capacitance changes - an index of vesicular exocytosis - at this site. Photoreceptors were voltage-clamped at -60mV, and stimulated with a 1 kHz sinusoidal voltage that delivered a 30mV peak-to-peak voltage change around the holding potential**.** HEKA software "Lock-in" mode was used to measure changes in membrane capacitance (C_m), access conductance (G_s) and membrane conductance (G_m) for each sine wave during the recordings. G_s and G_m did not significantly change during the C_m recordings, indicating a stable control.

Exocytosis was elicited by a 50ms depolarizing step from -60mV to -10mV, and C_m changes were measured 30 ms after the depolarizing step to avoid gating charges. A 30 sec interval separated the depolarizing pulses to allow photoreceptors to recover from the previous Ca^{2+} loading (Innocenti & Heidelberger, 2008). As shown in Figure 6A, the depolarizing voltage step elicited an increased C_m in both a rod and a cone in control conditions (black trace). This was slightly increased by application of 20μM glycine (Fig. 6A red trace). Results obtained from 24 rods and 16 cones are shown by the histograms (Fig. 6B). The data indicate that in control conditions the depolarizing pulse elicited an average increase of 116.1$\pm$ 7.2 fF in the C_m

recording in rods, and 167.2 $\pm$ 8.1 fF increase in cones. These values were further increased to 125 $\pm$ 4.3 fF and 175.3 $\pm$ 3.7 fF after applying glycine (Fig. 6B, blue bars), i.e., glycine increased the peak C_m about 9 $\pm$ 3.1 fF (n=24, $P< 0.05$) and 8 $\pm$ 4.4 fF (n=16, $P<0.05$) in rods and cones, respectively. Assuming that the fusion of a single vesicle at the synaptic terminal causes a capacitance increase of ~0.056 fF (Thoreson et al., 2004; Duncan et al., 2010), these capacitance changes demonstrate that glycine activation of the visual cells results in a rather small – but significant - increase in vesicle release.

Glycinergic feedback and the bipolar cell light response

The effects of strychnine on the light-evoked responses of ON-bipolar cells enabled us to demonstrate the regulation of signals between photoreceptors and ON-bipolar cells by endogenous glycine. Intracellular recordings were made on isolated intact retinas in order to avoid any loss of synaptic connections that occurs in the retinal slice. Using a series of intensities (controlled by the applied voltage) and 250ms duration from a white LED, it was possible to elicit a range of responses (from slightly above threshold to saturation) from ON-bipolar cells (Fig. 7A). When strychnine (2-5μM) was used to block the endogenous glycine input to bipolar cells, the amplitudes of the light-evoked responses were clearly reduced. The experiments were repeated on eight ON-bipolar cells. Intensity-response curves, plotted for the ON-bipolar cells, are shown in Fig. 7B. Subtracting the data recorded with strychnine (filled circles) from that obtained under control conditions (clear circles) yielded the net effect of endogenous glycine (triangles) on the ON-bipolar cells. The fact that the bipolar cell's response is smaller in the absence of glycine is a clear indication that endogenous glycine increases the response range of ON-bipolar cells.

The effects of endogenous glycine on light-evoked responses of OFF-bipolar cells were also studied with intracellular recordings in isolated intact retinas. The same light stimulus was used as in Fig. 7A. Strychnine reduced the amplitudes of the light-evoked responses (Fig. 7C). The experiments were repeated on nine OFF-bipolar cells. Among these recordings, strychnine decreased light responses in 7 of the OFF-bipolar cells, but had no apparent effect on 2 of the cells. Intensity response curves plotted from the seven OFF-bipolar cells are drawn in Fig. 7D. Subtracting the data recorded with strychnine (filled circles) from that obtained under control conditions (clear circles) illustrates the effect of endogenous glycine on the amplitude of the light-evoked voltage responses in OFF-bipolar cells.

Another series of paired electrode recordings from rods and OFF-bipolar cells in retinal slice preparation, using whole-cell patch-clamp techniques, yielded similar results, and provided further evidence that glycine increases the synaptic gain between photoreceptors and bipolar cells. A brief depolarizing step from -60mV to -10mV elicited glutamate release from the rods, and the currents generated were simultaneously recorded in OFF-bipolar cells that were voltage-clamped at -55mV, near the E_{Cl} of these neurons. Figure 8A shows the excitatory postsynaptic currents (EPSCs) in an OFF-bipolar cell in response to the 300ms stimulus (black trace). Glycine increased the EPSC (red trace), and its effect was completely blocked by strychnine (2 μM, green trace). These findings, replicated in recordings from four OFF-bipolar cells, provide evidence that glycine input in the distal retina can increase the synaptic input from rods to Off-bipolar cells. Similar results were obtained from cone-OFF bipolar cell pairs (Fig. 8B). Furthermore, in paired recordings from cones and OFF-bipolar cells, the inhibition of glutamate uptake by DHKA led to an increase in the peak and duration of the EPSCs and blocked the effect of glycine (Fig. 8C).

Modulation of the EPSCs by glycine and glycine with strychnine or DHKA was analyzed and expressed as the percentage change in the amount of positive charge transferred across the membrane. The results indicate that glycine increased by 44 $\pm$ 9% (n=4, $p<0.001$) the net charge in rod-evoked EPSCs; this effect was reduced to 12 $\pm$ 2% (n=3, $p<0.001$) by strychnine (Fig. 8D, left). Glycine also increased the charge transfer in cone-evoked EPSCs by 31 $\pm$ 6% (n=4, $p<0.005$). DHKA increased the EPSCs, and the charge was increased by about 87 $\pm$ 11% (n=4, $p<0.001$); in the presence of DHKA, glycine produced only a 9 $\pm$ 4% (n=4, $p<0.05$) charge increase (Fig. 8D, right).

In sum, the results of Figs. 7 and 8 are a good indication that glycine feedback in the OPL enhances light-evoked synaptic responses in both ON- and OFF-bipolar cells.

Discussion

There is an impressive array of events that regulate the discharge of at the photoreceptor terminal. They include the organization, anchoring and kinetics of Ca^{2+} channels in the active zones (Singer & Diamond, 2003; Thoreson et al., 2004; Jarsky et al., 2010; Scimemi & Diamond, 2012), the location and properties of release sites and the mechanism of vesicle trafficking (Tian et al., 2012; Nair et al., 2013; Chen et al., 2013), the biophysical requirements for synaptic membrane fusion (Ma et al., 2013), the turnover rate of synaptic vesicles (Babai et al, 2010; Van Hook & Thoreson, 2012), and the many factors that govern the tethering of vesicles to their active zones (cf. Li et al., 2011).

In addition, there are a number of ancillary processes that modulate transmitter release and affect the concentration of glutamate that enters the synaptic cleft. As reported in a prior publication (Rowan et al., 2010), uptake by a Na^+- and K^+- dependent membrane transporter, EAAT2A, responds rapidly to take up glutamate into photoreceptor terminals following release.

In the present study we reexamined the effect of the glycinergic feedback mechanism on the modulation of bipolar cell activity, and its effect on transmitter release and uptake in the dendrites of bipolar cells and the synaptic terminals of photoreceptors. We found that glycine enhances the synaptic gain between photoreceptors and bipolar cells by enhancing vesicle release, and suppressing glutamate uptake at these sites. These effects represent a novel mechanism by which interplexiform cells modulate intercellular signaling in the distal retina.

The analysis of glycinergic synapses on bipolar cell dendrites is not as straightforward as it seems, since there is an inhibitory input to the axon terminals of bipolar cells from glycinergic amacrine cells (Zhang et al., 1997; Lukasiewicz 2005; Hou et al., 2008). However, Maple & Wu (1998) found that bipolar cells have glycine receptors on their dendrites, and suggested that they are activated by glycinergic interplexiform cells. Our results from axon-truncated bipolar cells show more conclusively that glycine receptors are expressed on bipolar cell dendrites, and that they *are* activated by feedback from interplexiform cells. In salamander retina, bipolar cells are highly sensitive to a glycine input in the OPL (Wu & Maple, 1998). Thus glycine feedback from interplexiform cells is critical for regulation of bipolar cell membrane potentials.

Glycine receptors are expressed throughout the retina in various species. In tiger salamander retina, we have shown that this pentameric anion channel contains a GlyRα3 subunit. Although glycine receptors are abundantly expressed in both bipolar cells and horizontal cells in various species (Maple & Wu, 1998; Yazulla & Studholme 2001; Havekamp et al., 2003; Wassle et al., 2009; Vitanova, et al., 2004; Nobles et al., 2012), we have shown that in amphibian retina they represent postsynaptic receptors on bipolar cell dendrites, and receive synaptic inputs from glycinergic interplexiform cells. Although photoreceptors receive input from glycinergic interplexiform cells, their synaptic terminals are not labeled by a GlyRα3 antibody. Thus,

glycinergic synapses in photoreceptor terminals and bipolar cell dendrites might consist of different subtypes of glycine receptors with different binding affinities.

At this juncture, it is important to stress the relationship between photoreceptors and ON- and OFF-bipolar cells, as well as the effects of photic stimulation on these cell types. In darkness, for example, glutamate release is maximal, but it exerts different effects on the two classes of bipolar cell. Activation of the glutamate receptors on OFF-bipolar cells results in an ionotropic depolarizing response, whereas for ON-bipolar cells, the response is a hyperpolarizing response induced by a metabotropic mechanism. Interestingly, glycine depolarizes a group of ON-bipolar cells, but hyperpolarizes OFF-bipolar cells relative to their dark membrane potentials; these effects correspond to the typical light onset-induced membrane potential changes described above. Although the mechanism involved in the increased amplitude of the light responses in ON-bipolar cells is not addressed directly, the results of this study provide valuable information toward an understanding of the function of glycine in the modulation of signal transmission in bipolar cells. Consequently, light signals through ON and OFF pathways are enhanced by glycine feedback to the distal retina. Moreover, it appears that the effect of glycine regulation of glutamatergic synapses is probably minimal at light onset, since glutamate release in photoreceptors is reduced by light. Indeed, glycinergic regulation of glutamate uptake may be most effective at light offset, which produces a transient glutamate release.

It is noteworthy that studies in higher vertebrates have revealed the presence of a high Cl^- level in the somato-dendritic areas of ON-bipolar cells (Varela et al., 2005; Duebel et al., 2006). Since a similar situation exists in salamander retina, it is likely that the depolarizing effect of glycine on ON-bipolar cells is due to the high chloride reversal potential (E_{Cl}) in the bipolar cell dendrites, where glycine can cause a Cl^- efflux that induces cell depolarization (see Fig. 4).

Of particular interest is our finding that feedback by glycinergic interplexiform cells exerts two significant effects on the synaptic connectivity between photoreceptors and bipolar cells: (i) it acts directly on photoreceptors to produce a relatively small increase in the release of glutamatergic vesicles, and (ii) this effect is augmented by the ability of glycine to suppress glutamate uptake by photoreceptors. In both instances there results an increase in the glutamate concentration within the synaptic cleft and a concomitant enhancement in synaptic gain. Yet to be elucidated is precisely how the balance between the mechanisms that govern the reduction in glutamate release and those that promote an increase in transmitter release are maintained to produce a precise and tunable physiological response.

References

Arriza JL, Eliasof S, Kavanaugh MP & Amara SG (1997). Excitatory amino acid transporter 5, a retinal glutamate transporter coupled to a chloride conductance. *Proc Natl Acad Sci U SA,* **94**, 4155-4160.

Babai N, Morgans CW & Thoreson WB (2010). Calcium-induced calcium release contributes to synaptic release from mouse rod photoreceptors. *Neurosci.,* 165(4):1447-56.

Dowling JE & Ehinger B (1978). The interplexiform cell system. I. Synapses of the dopaminergic neurons of the goldfish retina. *Proc R Soc Lond B Biol Sci.,* 201:7-26.

Duebel J, Haverkamp S, Schleich W, Feng G, Augustine GJ, Kuner T & Euler T (2006). Two-photon imaging reveals somatodendritic chloride gradient in retinal ON-type bipolar cells expressing the biosensor Clomeleon. *Neuron.* 49: 81-94.

Duncan G, Rabl K, Gemp I, Heidelberger R & Thoreson WB（ 2010). Quantitative analysis of synaptic release at the photoreceptor synapse. *Biophys J*., 98(10):2102-10.

Eliasof S, Arriza JL, Leighton BH, Kavanaugh MP & Amara SG (1998). Excitatory amino acid transporters of the salamander retina: identification, localization, and function. *J Neurosci* 18, 698-712.

Famiglietti EV& Kolb H (1976). Structural basis for ON- and OFF-center responses in retinal ganglion cells. *Science*. 194:193–195.

Haverkamp S, Muller U, Harvey K, Harvey RJ, Betz H, & Wassle H (2003). Diversity of glycine receptors in the mouse retina: localization of the alpha3 subunit. *J Comp Neurol* **465**, 524-539.

Hou M, Duan L & Slaughter MM (2008). Synaptic inhibition by glycine acting at a metabotropic receptor in tiger salamander retina. *J. Physiol.* 586(12):2913-26.

Innocenti B & Heidelberger R (2008). Mechanisms contributing to tonic release at the cone photoreceptor ribbon synapse. *J. Neurophysiol* **99**, 25-36 2008.

Jarsky T, Tian M & Singer JH (2010). Nanodomain control of exocytosis is responsible for the signaling capability of a retinal ribbon synapse. *J. Neurosci.*, 30:11885-11895.

Jiang Z & Shen W (2010). Role of neurotransmitter receptors in mediating light-evoked responses in retinal interplexiform cells. *J. Neurophysiol.*, 103:924-933.

Li W, Ma C, Guan R, Xu Y, Tomchick DR & Rizo J (2011). The crystal structure of a Munc13 C-terminal module exhibits a remarkable similarity to vesicle tethering factors. *Structure*. 19:1443-1455.

Lukasiewicz PD (2005). Synaptic mechanisms that shape visual signaling at the inner retina. *Prog Brain Res* **147**, 205-218.

Ma C, Su L, Seven AB, Xu Y, Rizo J. (2013) Reconstitution of the vital functions of Munc18 and Munc13 in neurotransmitter release. *Science* **339**:421-5.

Mangel SC & Dowling JE (1987). The interplexiform-horizontal cell system of the fish retina: effects of dopamine, light stimulation and time in the dark. *Proc R Soc Lond B Biol Sci* **231**, 91-121.

Maguire G, Lukasiewicz P, & Werblin F. (1990). Synaptic and voltage-gated currents in interplexiform cells of the tiger salamander retina. *J Gen Physiol* **95**, 755-770.

Maple BR & Wu SM. (1998). Glycinergic synaptic inputs to bipolar cells in the salamander retina. *J Physiol* **506 (Pt 3)**, 731-744.

Nair R, Lauks J, Jung SY, Cooke NE, de Wit H, Brose N, Kilimann MW, Verhage M & Rhee JS (2013). Neurobeachin regulates neurotransmitter receptor trafficking to synapses. *J Cell Biol*., 200: 61-80,

Nobles RD, Zhang C, Müller U, Betz H & McCall MA (2012). Selective glycine receptor α2 subunit control of crossover inhibition between the on and off retinal pathways. *J Neurosci.,* 32(10):3321-32.

Otis TS & Jahr CE (1998). Anion currents and predicted glutamate flux through a neuronal glutamate transporter. *J Neurosci* **18**, 7099-7110.

Pang JJ, Gao F & Wu SM (2004). Stratum-by-stratum projection of light response attributes by retinal bipolar cells of ambystoma. J Physio., 558(1):249-262.

Rowan MJ, Ripps H & Shen W (2010). Fast glutamate uptake via EAAT2 shapes the cone-medicated light offset response in bipolar cells. *J Physiol.,* 588:3943-3956.

Scimemi, A & Diamond, JS (2012). The number and organization of Ca^{2+} channels in the active zone shapes neurotransmitter release from Schaffer collateral synapses, J. Neurosci. 32, 18157-18176.

Shen W, Jiang Z & Li B (2008). Glycine input induces the synaptic facilitation in salamander rod photoreceptors. *J Biomed Sci*., 15:743-754.

Singer JH & Diamond JS (2003). Sustained Ca^{2+} entry elicits transient postsynaptic currents at a retinal ribbon synapse. *Neuroscience* 23:10923-10933.

Smiley JF & Basinger SF. (1988). Somatostatin-like immunoreactivity and glycine high-affinity uptake colocalize to an interplexiform cell of the Xenopus laevis retina. *J Comp Neurol.,* **274**, 608-618.

Thoreson WB, Rabl K, Townes-Anderson E & Heidelberger R (2004). A highly Ca2+-sensitive pool of vesicles contributes to linearity at the rod photoreceptor ribbon synapse. *Neuron.* 42(4):595-605.

Tian M, Xu CS, Montpetit R & Kramer RH (2013). Rab3A mediates vesicle delivery at photoreceptor ribbon synapses. *J Neurosci.* 32(20): 6931–6936

Van Hook MJ & Thoreson WB (2012). Rapid synaptic vesicle endocytosis in cone photoreceptors of salamander retina. *J Neurosci*., 32(50):18112-23.

Van Hook, MJ., Thoreson, WB (2013) Simultaneous Whole-cell Recordings from Photoreceptors and Second-order Neurons in an Amphibian. Retinal Slice Preparation. J. Vis. Exp. (76): Pub Med, on line.

Varela C, Blanco R & De la Villa P (2005). Depolarizing effect of GABA in rod bipolar cells of the mouse retina. *Vis. Res.,* 45:2659-2667.

Vitanova L Haverkamp S & Wassle H (2004). Immunocytochemical localization of glycine and glycine receptors in the retina of the frog Rana ridibunda. *Cell Tissue Res.,* 317:227-235.

Wallace BA (1986). Structure of gramicidin A. *Biophys J.*, 49:295-306.

Wassle H, Heinze L, Ivanova E, Majumdar S, Weiss J, Harvey R & Haverkamp S (2009). Glycinergic transmission in the mammalian retina. *Frontiers in Nolecular Neuroscei*., July Vol 2, Article 6.

Wu SM & Maple BR (1998). Amino Acid neurotransmitters in the retina: a functional overview. *Vision Research,* 38:1371-1384.

Yang CY & Yazulla S (1988). Light microscopic localization of putative glycinergic neurons in the larval tiger salamander retina by immunocytochemical and autoradiographical methods. *J Comp Neurol* **272**, 343-357.

Yazulla, S & Studholme, KM (2001). Neurochemical anatomy of the zebrafish retina as determined by immunocytochemistry *J. Neurocytol.* 30(7):551-592

Zhang J, Jung CS & Slaughter MM (1997). Serial inhibitory synapses in retina. *Vis Neurosci.* 14(3):553-63.

Author contributions:

Z.J., H.R. and W.S. contributed to the design of the study. Z.J., J.N.Y., L.A.P. and W.S. performed the electrophysiological experiments, Y.F.L. contributed antibody labeling data, H.R. and W.S. analyzed data and wrote the paper with input from all authors. The study was completed at Florida Atlantic University

Acknowledgements:

This study was supported by grants from the National Science Foundation (NSF, IOS-1021646, WS) and the National Eye Institute (NEI, EY 14161, WS).

Figure Legends

Figure 1. Localization and voltage response of a glycinergic interplexiform cell. ***A,*** The schematic drawing illustrates the location of the interplexiform cell and its extended processes. ***B,*** Current clamp recording shows the voltage responses of an interplexiform cell to the onset and offset of a 3 sec green (520 nm) stimulus.

Figure 2. Glycine-induced synaptic currents recorded from axon-truncated ON-bipolar cells. ***A,*** The axon-truncated ON-bipolar cell in the dark-adapted retinal slice preparation following Lucifer Yellow staining. The experimental procedure is depicted in the schematic drawing below. ***B,*** The synaptic currents recorded from an axon-truncated cell held at 0mV in response to focal application of 1mM glutamate at the IPL. The initial currents were completely suppressed by strychnine, and partially recovered after washout. C, The inset boxes from B in an extended time scale.

Figure 3. Expression of the glycine receptor subunit (GlyRα3). ***A,*** The three panels show a retinal section labeled with GlyRα3, $G_{o\alpha}$ (an ON-bipolar cell marker), and an overlay of the two images showing sparse co-localization (yellow areas) in the OPL. ***B,*** The anti-GlyRα3 labels OFF-bipolar cells in the salamander retina. ***C,*** Western blots showing that the GlyRα3 antibody binds specifically to 46 kDa and 48 kDA proteins in salamander and mouse retinal samples, respectively. ***D,*** The anti-GlyRα3 and anti-calretinine, a horizontal cell marker, label different cells in the distal retina.

Figure 4. Gramicidin perforated-patch recording of glycine current reversal potentials in the somato-dendritic areas of ON- and OFF-bipolar cells. ***A,*** Morphology of a rod-dominated ON-bipolar cell with axon terminal ending at the border of sublamina *b* of the IPL, marked by Lucifer Yellow; glycine elicited currents in the neuron when it was voltage-clamped at various potentials as indicated. ***B,*** A summary of glycine current reversal potentials recorded from rod-dominated ON-bipolar cells. ***C &D***, Glycine-elicited currents recorded from ON-bipolar cells. ***E &F,*** Glycine currents recorded from OFF-bipolar cells.

Figure 5. Glycine suppresses glutamate uptake via EAAT2. ***A,*** The EAAT current elicited by a brief depolarizing step was blocked by DHKA, the selective inhibitor of EAAT2. ***B,*** Glycine also suppressed most of the EAAT current. ***C,*** DHKA completely blocked the effect of glycine in a rod. ***D,*** Strychnine (10μM) blocked the effect of glycine on the EAAT current. ***E,*** Histograms illustrate average suppression of EAAT currents in rods by glycine and glycine with either strychnine or DHKA, error bars show means $\pm$ SEM. ***F & G,*** Glycine suppressed EAAT current in a cone and the effect was blocked by DHKA. ***H,*** Histograms showing the average suppression of EAAT currents by glycine with and without DHKA in cones.

Figure 6. **Glycine enhances the release of synaptic vesicles.** ***A,*** The effects of glycine on capacitance changes in rods and cones activated by a 50ms depolarizing voltage step. ***B,*** Averaged changes in peak capacitance induced by glycine in rods and cones; error bars show mean $\pm$ SEM. In both cases the changes were significant ($p<0.05$)

Figure 7. Strychnine reduces the amplitudes of light-evoked response in bipolar cells . ***A&C,*** Intracellular recording of light-evoked responses from ON- and OFF-bipolar cells. The

cells were stimulated by a range of intensities (between 0.6 lux to 2.4 lux) that generated a graded series of responses. Strychnine reduced the light response of bipolar cells. ***B&D,*** The intensity-response curves generated from ON- and OFF-bipolar cells (n=5) in control and strychnine. Subtraction of the two curves (triangles) reveals the enhancement of light-evoked responses by endogenous glycine.

Figure 8. Glycine increases EPSCs in OFF bipolar cells. ***A,*** Paired recording of a rod and OFF-bipolar cell; a brief depolarizing pulse to the rod evoked an EPSC in the OFF-bipolar cell; glycine increased the amplitude of the EPSCs, but the effect was completely blocked by strychnine. ***B,*** Paired recording of a cone and OFF-bipolar cell; glycine increased the peak amplitude of the EPSC in the OFF-bipolar cell. ***C,*** DHKA inhibited glutamate uptake resulting in an increased amplitude of the EPSC in the OFF-bipolar cell; with DHKA, glycine produced a slight increase in the ESPC. ***D,*** Bar graphs show the averaged charge transfer across the bipolar cell membrane in EPSCs evoked by depolarizing rods and cones. Glycine, strychnine and DHKA modulate the magnitude of the positive charge; glycine increased by 44 $\pm$ 9% (n=4) the charge influx in the rod-evoked EPSCs; in the presence of strychnine, the increase was only 12 $\pm$ 2% (n=3). Glycine also increased the charge influx by 31 $\pm$ 6% (n=4) in cone-generated EPSCs; DHKA increased the charge influx in EPSCs by 87 $\pm$ 11% (n=4), whereas the amount of charge transferred was increased by only in 9 $\pm$ 4% (n=4) when glycine was applied in the presence of DHKA (right). * $p<0.001$; ** $p<0.005$; *** $p<0.05$.

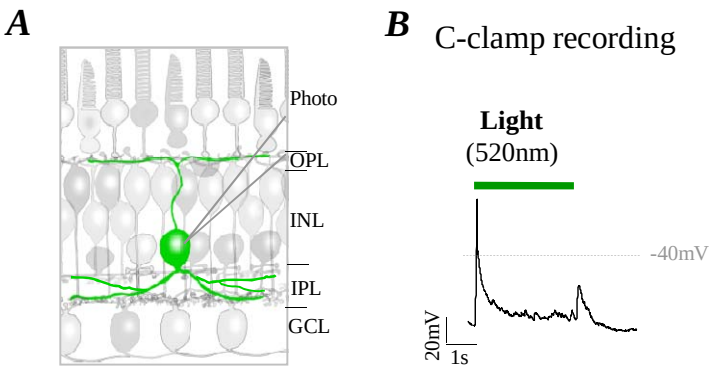

Figure 1. Localization and voltage response of a glycinergic interplexiform cell. ***A,*** This schematic drawing illustrates the location of the interplexiform cell and its extended processes. ***B,*** Current clamp recording shows the voltage responses of an interplexiform cell to the onset and offset of a 3 sec green (520 nm) stimulus..

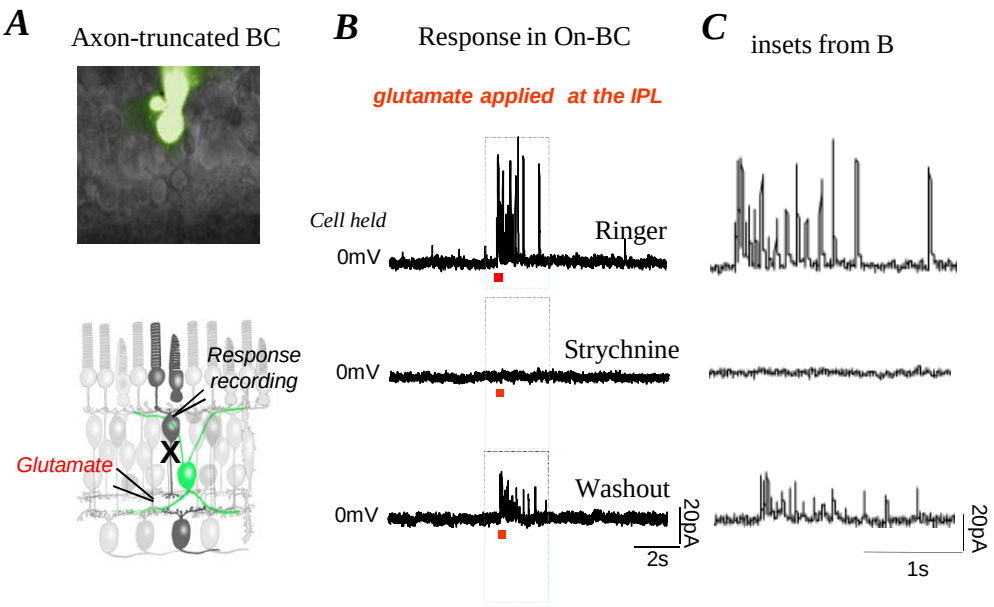

Figure 2. Glycine-induced synaptic currents recorded from axon-truncated ON-bipolar cells. ***A,*** The axon-truncated ON-bipolar cell in the dark-adapted retinal slice preparation following Lucifer Yellow staining. The experimental procedure is depicted in the schematic drawing below. ***B,*** The synaptic currents recorded from an axon-truncated cell held at 0mV in response to a focal application of 1mM glutamate at the IPL. The initial currents were completely suppressed by strychnine, and partially recovered after washout. ***C,*** The inset boxes from ***B*** in an extended time scale**.**

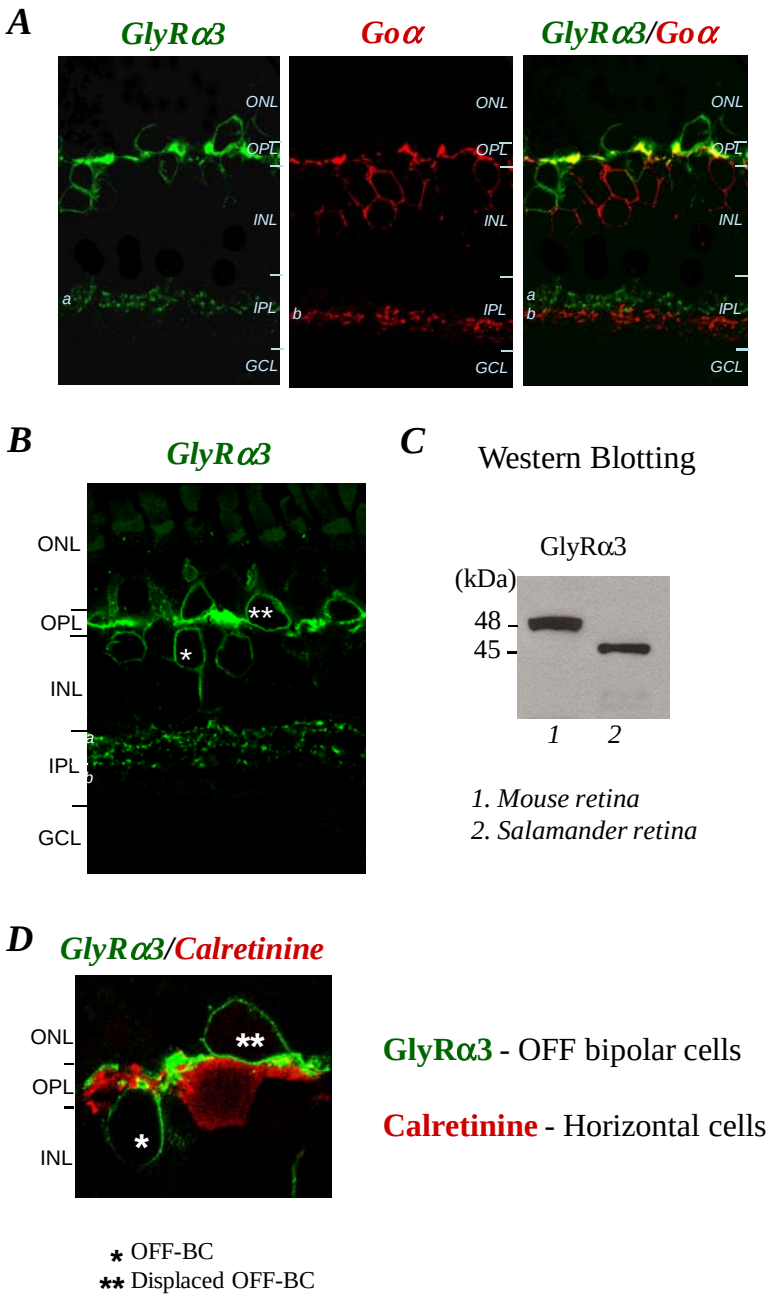

Figure 3. Expression of the glycine receptor subunit (GlyRα3). ***A,*** The three panels show a retinal section labeled with GlyRα3, Goα (an ON-bipolar cell marker), and an overlay of the two images showing sparse co-localization (yellow areas) in the OPL. ***B,*** The anti-GlyRα3 labels OFF-bipolar cells in the salamander retina. ***C,*** Western blots showing that the GlyRα3 antibody binds specifically to 46 kDa and 48 kDA proteins in salamander and mouse retinal samples, respectively. ***D,*** The anti-GlyRα3 and anti-calretinine, a horizontal cell marker, label different cells in the distal retina.

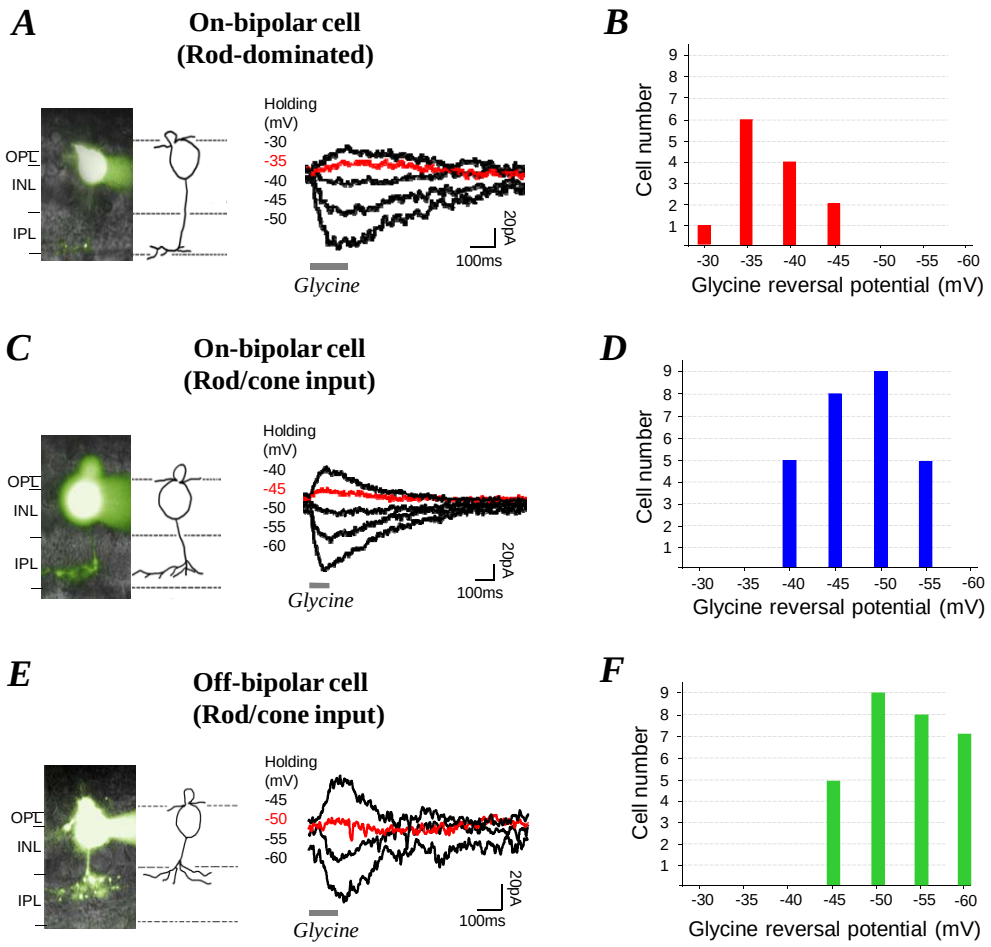

Figure 4. Gramicidin perforated-patch recording of glycine current reversal potentials in the somato-dendritic areas of ON- and OFF-bipolar cells. ***A,*** Morphology of a rod-dominated ON-bipolar cell with axon terminal ending at the border of sublamina *b* of the IPL, marked by Lucifer Yellow; glycine elicited currents in the neuron when it was voltage-clamped at various potentials as indicated. ***B,*** A summary of glycine current reversal potentials recorded from rod-dominated ON-bipolar cells. ***C&D***, Glycine-elicited currents were recorded from ON-bipolar cells. ***E&F,*** Glycine currents recorded from OFF-bipolar cells.

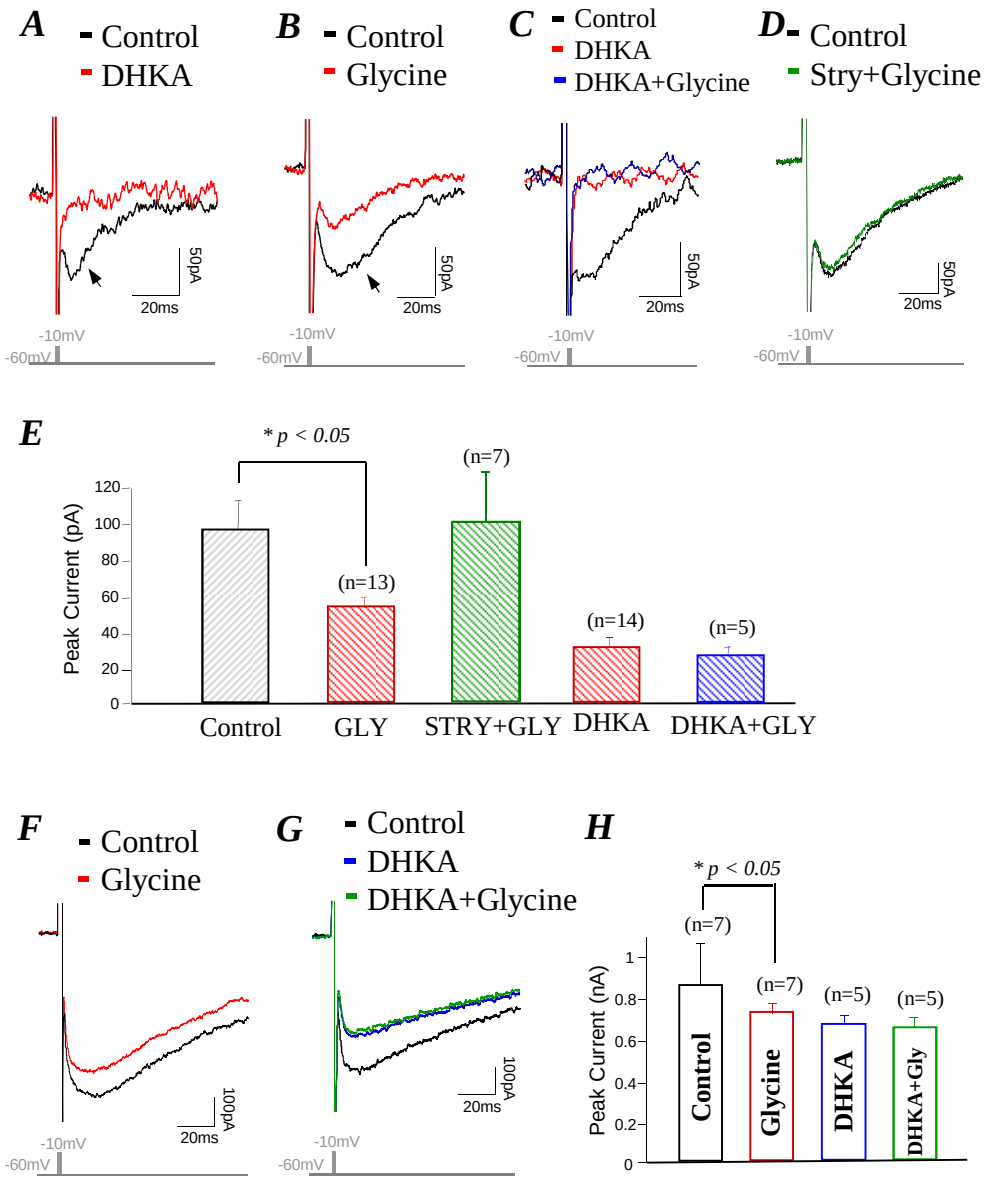

Figure 5. Glycine suppresses glutamate uptake via EAAT2. ***A,*** The EAAT current elicited by a brief depolarizing step was blocked by DHKA, the selective inhibitor of EAAT2. ***B,*** Glycine also suppressed most of the EAAT current. ***C,*** DHKA completely blocked the effect of glycine in a rod. ***D,*** Strychnine (10μM) blocked the effect of glycine on the EAAT current. ***E,*** Histograms illustrate average suppression of EAAT currents in rods by glycine and glycine with either strychnine or DHKA, error bars show means ± SEM. ***F & G,*** Glycine suppressed EAAT current in a cone and the effect was blocked by DHKA. ***H,*** Histograms of average suppressions of EAAT currents by glycine with and without DHKA in cones.

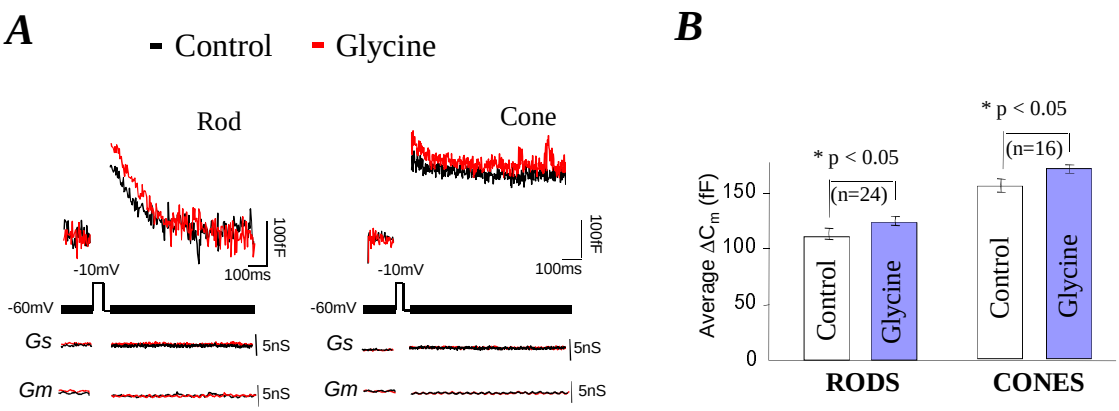

Figure 6. **Glycine enhances the release of synaptic vesicles.** ***A,*** The effects of glycine on capacitance changes in rods and cones activated by a 50ms depolarizing voltage step. ***B,*** Averaged changes in peak capacitance induced by glycine in rods and cones; error bars show mean $\pm$ SEM. In both cases the changes were significant ($p<0.05$)

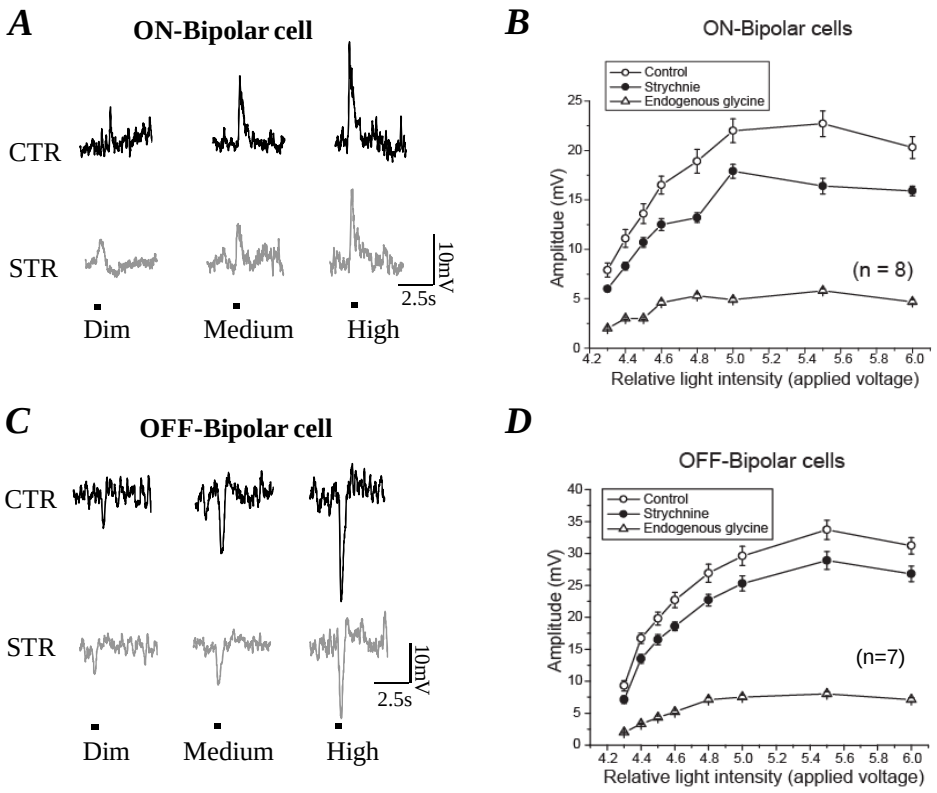

Figure 7. Strychnine reduces the amplitudes of light-evoked response in bipolar cells. ***A&C,*** Intracellular recording of light-evoked responses from ON- and OFF-bipolar cells. The cells were stimulated by a range of intensities that generated a graded series of responses. Strychnine reduced the light response of bipolar cells. ***B&D,*** The intensity-response curves generated from ON- and OFF-bipolar cells (n=5) in control and strychnine. Subtraction of the two curves (triangles) reveals the enhancement of light-evoked responses by endogenous glycine.

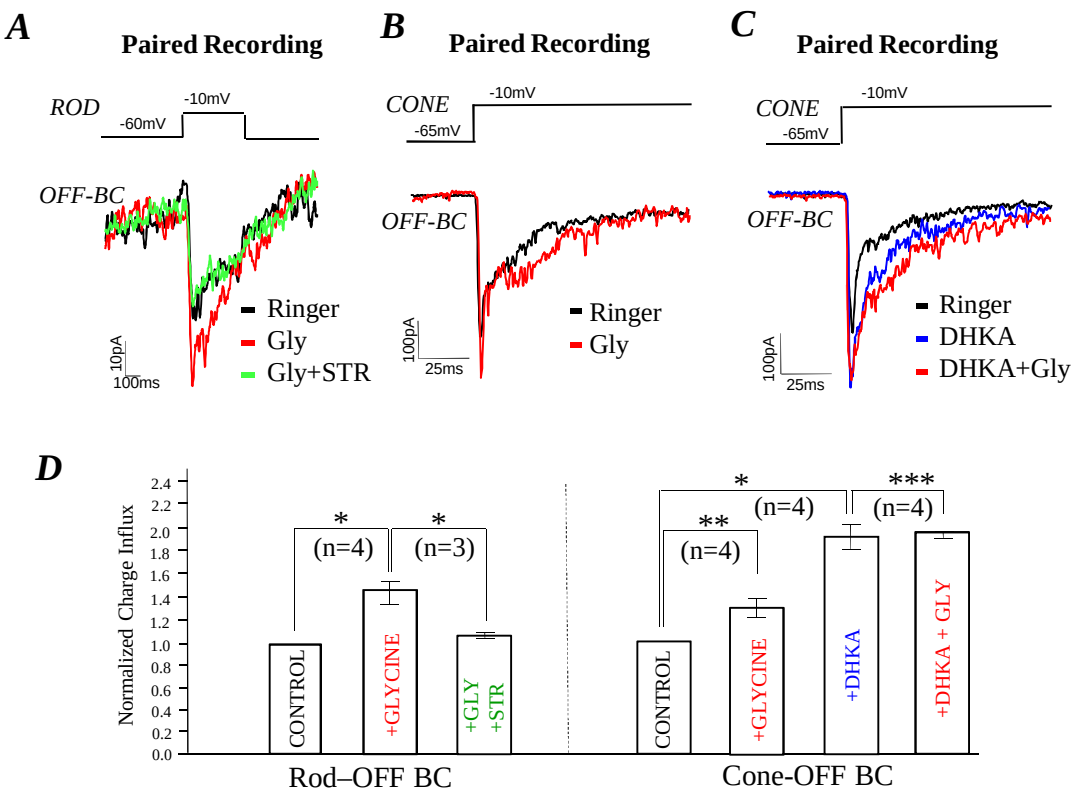

Figure 8. Glycine increases EPSCs in OFF bipolar cells. ***A,*** Paired recording of a rod and OFF-bipolar cell; a brief depolarizing pulse to the rod evoked an EPSC in the OFF-bipolar cell; glycine increased the amplitude of the EPSCs, but the effect was completely blocked by strychnine. ***B,*** Paired recording of a cone and OFF-bipolar cell; glycine increased the peak amplitude of the EPSC in the OFF-bipolar cell. ***C,*** DHKA inhibited glutamate uptake resulting in an increased amplitude of the EPSC in the OFF-bipolar cell; with DHKA, glycine produced a slight increase in the ESPC**.** ***D,*** Bar graphs show the averaged charge transfer across the bipolar cell membrane in EPSCs evoked by depolarizing rods and cones. Glycine, strychnine and DHKA modulate the magnitude of the positive charge; glycine increased by 44 $\pm$ 9% (n=4) the charge influx in the rod-evoked EPSCs; in the presence of strychnine, the increase was only 12 $\pm$ 2% (n=3). Glycine also increased the charge influx by 31 $\pm$ 6% (n=4) in cone-generated EPSCs; DHKA increased the charge influx in EPSCs by 87 $\pm$ 11% (n=4), whereas the amount of charge transferred was increased by only in 9 $\pm$ 4% (n=4) when glycine was applied in the presence of DHKA (right). * $p<0.001$; ** $p<0.005$; ***$p<0.05$.